Hindawi
Discrete Dynamics in Nature and Society
Volume 2020, Article ID 2149037, 13 pages
https://doi.org/10.1155/2020/2149037

Research Article

Numerical Solution of Fractional-Order HIV Model Using Homotopy Method

Sami Aljhani,[1] **Mohd Salmi Md Noorani**,[1] **and A. K. Alomari**[2]

[1]*Department of Mathematical Sciences, Faculty Science and Technology, Universiti Kebangsaan Malaysia, 43600 UKM, Bangi, Selangor, Malaysia*
[2]*Department of Mathematics, Faculty of Science, Yarmouk University, 211-63 Irbid, Jordan*

Correspondence should be addressed to Sami Aljhani; sami.aljhani@gmail.com

Received 30 January 2020; Revised 23 February 2020; Accepted 24 February 2020; Published 15 April 2020

Guest Editor: Qasem M. Al-Mdallal

In this study, we construct a convergent algorithm for generating an approximate analytic solution for the fractional HIV infection of $CD4^+$ T cells with Atangana–Baleanu fractional derivatives in the Caputo sense. We compute the solution by utilizing the fractional homotopy analysis transform method (FHATM) and achieved a convergence region of the solution by employing an auxiliary parameter. Moreover, we apply a numerical scheme proposed by Toufik and Atangana for solving this kind of problem and compared with our results. A good agreement between the new algorithm and the numerical scheme is remarkable. The solution via the present algorithm can be obtained without any linearization or discretization which makes it reliable and easy to apply.

1. Introduction

Fractional calculus has played a significant role within the field of science and engineering, and many mathematicians and scientists have been working in this field lately. In recent decades, fractional calculus has been used in several areas of physics, biology, engineering, and others. Further details about fractional calculus and its applications can be found in the literature [1–9].

Because most nonlinear fractional differential equations cannot be solved exactly, it is necessary to use approximate and numerical methods. Various powerful mathematical techniques such as the Adomian decomposition method (ADM) [10, 11], homotopy analysis method (HAM) [12–15], optimal homotopy asymptotic method (OHAM) [16], homotopy perturbation method (HPM) [17], and variational iterative method (VIM) [18, 19] have been used to obtain an exact and approximate analytical solution.

The HAM was first introduced and employed in 1992 by Liao [20], after which many researchers successfully applied this method to solve linear and nonlinear differential equations. In recent years, many researchers have devoted their attention to obtaining a solution of linear and nonlinear differential equations using a variety of methods based on Laplace transform such as the Laplace decomposition method (LDM) [21] and the homotopy perturbation transform method (HPTM) [22]. Khan et al. [23] and Kumar et al. [24–26] coupled the HAM with Laplace transform to solve a nonlinear differential equation and Volterra integral equation. The homotopy analysis transform method (HATM) is a combination of HAM with Laplace transformation. The main advantage of this method is its ability to combine two powerful methods to obtain a rapid convergent series for fractional differential equations. This method provides us with a convenient way to control the convergence of the series solution.

Recently, Toufik and Atangana [27] developed a numerical scheme to solve a nonlinear fractional differential equation considering the Atangana–Baleanu fractional derivative. This method is a combination of the fundamental fractional calculus theorem with two-step Lagrange polynomial which is successfully used to solve many real-world problems [28–30].

Since the early 1980s, researchers have made an enormous effort to mathematically model the human immunodeficiency virus (HIV), the virus responsible for causing acquired immune deficiency syndrome (AIDS). In 1989,

Perelson [31] considered the interaction of uninfected (T) and infected CD4$^+$ (I) T cells, and free virus molecules (F) in his model, following which Perelson et al. [32] extended the original model [31]. Culshaw and Ruan [33] reduced the model discussed in [32] as follows:

$$\frac{dT}{dt} = p - \mu_T T + kT\left(1 - \frac{T+I}{T_{\max}}\right) - k_1 FT, \tag{1}$$

$$\frac{dI}{dt} = k_1' FT - \mu_I I, \tag{2}$$

$$\frac{dF}{dt} = M\mu_b I - k_1 FT - \mu_F F, \tag{3}$$

where $T(t)$, $I(t)$, and $F(t)$ represent the concentration of healthy CD4$^+$ T cells at time t, infected CD4$^+$ T cells, and the free HI virus at time t, respectively. Table 1 summarizes the meanings of functions and parameters. Equation (1) describes the rate of change in the uninfected population of CD4$^+$ T cells. The first term is the constant rate at which the body produces CD4$^+$ T cells from precursors in the bone marrow. Because the virus can infect both thymocytes and T cells, as for all cells in the body, these cells have a finite lifetime; thus, the second term describes the decreasing source. The third term describes the logistic growth of the healthy CD4$^+$ T cells, and the proliferation of infected CD4$^+$ T cells is neglected. The last term models the rate at which the free virus infects a CD4$^+$ T cell. Once a T cell has been infected, it becomes an infected cell; therefore, k_1 FT is subtracted from equations (1) and (3) and added to equation (2). Hence, F and T decrease concurrently.

Equation (2) describes the rate of change in the infected population of actively infected T cells. The first term represents the rate of infection of CD4$^+$ T cells by the virus. The second term represents the rate of disappearance of infected cells.

The three terms in equation (3) refer to the rate of production and destruction of the free infection virus. An actively infected CD4$^+$ T cell produces M virus particles; thus, the rate at which the virus is produced is set equal to M times the lytic death rate for the infected cell. A free virus is lost as a result of binding to an uninfected CD4$^+$ T cell at k_1 FT. The third term accounts for the loss of viral infectivity, viral death, and/or clearance from the body.

In this study, our approach to solving the fractional HIV model is to determine the order in which the fractional derivative changes by extending the classical HIV model (1)–(3) to the following set of fractional ordinary differential equations of the order α, β, and γ:

$${}_a^{\mathrm{ABC}}D_t^{\alpha} T(t) = p - \mu_T T + kT\left(1 - \frac{T+I}{T_{\max}}\right) - k_1 FT, \quad 0 < \alpha < 1, \tag{4}$$

$${}_a^{\mathrm{ABC}}D_t^{\beta} F(t) = k_1' FT - \mu_I I, \quad 0 < \beta < 1, \tag{5}$$

Table 1: List of parameters and functions.

Parameters and functions	Description	Values
$T(t)$	Concentration of uninfected CD4$^+$ T cells	$T(0) = 1000$
$I(t)$	Concentration of infected CD4$^+$ T cells	$I(0) = 0$
$F(t)$	Concentration of HIV RNA	$F(0) = 0.001$
μ_T	Natural death rate of CD4$^+$T cells (concentration)	0.02
μ_I	Blanket death rate of infected CD4$^+$ T cells	0.26
μ_b	Lytic death rate of infected cells	0.24
μ_F	Death rate of free virus	2.4
k_1	Rate at which CD4$^+$ T cells become infected with the virus	2.4×10^{-5}
k_1'	Rate at which infected cells become active	2×10^{-5}
k	Growth rate of concentration of CD4$^+$ T cells	0.03
M	Number of virion produced by infected CD4$^+$ T cells	500
$T_{\max}$	Maximal concentration of CD4$^+$ T cells	1500
p	Source term for uninfected CD4$^+$ T cells	10

$$F(t) = M\mu_b I - k_1 FT - \mu_F F, \quad 0 < \gamma < 1, \tag{6}$$

with initial conditions

$$\begin{aligned} T(0) &= T_0(0), \\ I(0) &= I_0(0), \\ F(0) &= F_0(0), \end{aligned} \tag{7}$$

where ${}_a^{\mathrm{ABC}}D_t^{\alpha}$, ${}_a^{\mathrm{ABC}}D_t^{\beta}$, and ${}_a^{\mathrm{ABC}}D_t^{\gamma}$ are the Atangana–Baleanu fractional derivative in the Caputo sense (ABC). To the best of our knowledge, this is the first work that solves fractional HIV infection of the CD4$^+$ T cells model in ABC sense analytically and numerically. To indicate the strength of our proposed method, we compare our findings with the algorithm of Toufik and Atangana [27].

2. Preliminaries and Notations

The Atangana–Baleanu fractional derivative in the Caputo sense (ABC) is defined as [6, 34]

$${}_a^{\mathrm{ABC}}D_t^{\alpha} f(t) = \frac{M(\alpha)}{1-\alpha} \int_a^t \frac{d}{dt} f(s) \mathbf{E}_{\alpha}\left(\frac{-\alpha}{1-\alpha}(t-s)^{\alpha}\right) ds, \quad n-1 < \alpha \le n, \tag{8}$$

where $\alpha \in \mathbb{R}$, $M(\alpha) > 0$ is a normalization function satisfying

$$M(\alpha) = (1-\alpha) + \frac{\alpha}{\Gamma(\alpha)}, \tag{9}$$

with $M(0) = M(1) = 1$, $\mathbf{E}_{\alpha}(\cdot)$ denotes the Mittag-Leffler function, defined by

$$\mathbf{E}_{\alpha}(z) = \sum_{k=0}^{\infty} \frac{z^k}{\Gamma(\alpha k + 1)}, \tag{10}$$

and $\Gamma(\cdot)$ denotes Euler's gamma function defined as

$$\Gamma(z) = \int_0^{\infty} t^{z-1} e^{-t} \mathrm{d}t, \quad \Re(z). \tag{11}$$

The fractional integral for the ABC, which is newly defined with a nonlocal kernel and does not have singularities at $t = s$, is defined as follows [6]:

$${}^{\mathrm{ABC}}_{a}I^{\alpha}_{t} f(t) = \frac{1-\alpha}{M(\alpha)} f(t) + \frac{\alpha}{M(\alpha)\Gamma(\alpha)} \int_a^t f(s)(t-s)^{\alpha-1} \mathrm{d}s. \tag{12}$$

Here, when α equals zero, the initial function is recovered, and when α equals unity, the classical ordinary integral is obtained.

The Laplace transform of the fractional definitions with ABC is given as follows [6]:

$$\mathscr{L}\left\{{}^{\mathrm{ABC}}_{a}D^{\alpha}_{t} f(t)\right\}(s) = \left(\frac{M(\alpha)}{1-\alpha} \frac{s^{\alpha}\mathscr{L}\{f(t)\}(s) - s^{\alpha-1} f(a)}{s^{\alpha} + (\alpha/1-\alpha)}\right). \tag{13}$$

3. Homotopy and Laplace Transform for FHATM

Applying the Laplace transform to equations (4)–(6) and using the formula for the Laplace transform of the ABC and then simplifying these equations, we find that

$$\begin{aligned}
\mathscr{L}\{T(t;q)\} &= \frac{T(0)}{s} + \frac{p}{s}\frac{s^{\alpha}(1-\alpha)+\alpha}{s^{\alpha}M(\alpha)} + \frac{s^{\alpha}(1-\alpha)+\alpha}{s^{\alpha}M(\alpha)} \\
&\quad \cdot \left(\mathscr{L}(k-\mu_T)T(t) - \frac{k}{T_{\max}}(T(t))^2 - \frac{k}{T_{\max}} T \right. \\
&\quad \left. \cdot (t)I(t) - k_1 F(t)T(t)\right), \\
\mathscr{L}\{I(t;q)\} &= \frac{I(0)}{s} + \frac{s^{\beta}(1-\beta)+\beta}{s^{\beta}M(\beta)}\mathscr{L}\{k_1' F(t)T(t) - \mu_I I(t)\}, \\
\mathscr{L}\{F(t;q)\} &= \frac{F(0)}{s} + \frac{s^{\gamma}(1-\gamma)+\gamma}{s^{\gamma}M(\gamma)}\mathscr{L}\{M\mu_b T(t) - k_1 F(t)T(t) \\
&\quad - \mu_F F(t)\}.
\end{aligned} \tag{14}$$

Next, defining the nonlinear operators as

$$\begin{aligned}
N_T[\varphi_1(t;q), \varphi_2(t;q), \varphi_3(t;q)] &= \mathscr{L}[\varphi_1(t;q)] - \frac{T(0)}{s} - \frac{p}{s}\frac{s^{\alpha}(1-\alpha)-\alpha}{s^{\alpha}M(\alpha)} - \frac{s^{\alpha}(1-\alpha)+\alpha}{s^{\alpha}M(\alpha)}\mathscr{L} \\
&\quad \cdot \left\{\left((k-\mu_T)\varphi_1(t;q); -\frac{k}{T_{\max}}(\varphi_1(t;q))^2 - \frac{k}{T_{\max}}\varphi_1(t;q)\varphi_2(t;q) - k_1\varphi_3(t;q)\varphi_1(t;q)\right)\right\}, \\
N_I[\varphi_1(t;q), \varphi_2(t;q), \varphi_3(t;q)] &= \mathscr{L}[\varphi_2(t;q)] - \frac{I(0)}{s} - \frac{s^{\beta}(1-\beta)+\beta}{s^{\beta}M(\beta)}\mathscr{L}\{k_1'\varphi_3(t;q)\varphi_1(t;q) - \mu_I\varphi_2(t;q)\}, \\
N_F[\varphi_1(t;q), \varphi_2(t;q), \varphi_3(t;q)] &= \mathscr{L}[\varphi_3(t;q)] - \frac{F(0)}{s} - \frac{s^{\gamma}(1-\gamma)+\gamma}{s^{\gamma}M(\gamma)}\mathscr{L}\{M\mu_b\varphi_1(t;q) - k_1\varphi_3(t;q)\varphi_1(t;q) - \mu_F\varphi_3(t;q)\},
\end{aligned} \tag{15}$$

where N_T, N_I, and N_F are the nonlinear operators. Let $\hbar$ be a nonzero auxiliary parameter. Using the embedding parameter $q \in [0,1]$, we construct the so-called zeroth-order deformation equation:

$$(1-q)\mathscr{L}[\varphi_1(t;q) - T_0(t)] = q\hbar N_1[\varphi_1(t;q), \varphi_2(t;q), \varphi_3(t;q)], \tag{16}$$

$$(1-q)\mathscr{L}[\varphi_2(t;q) - I_0(t)] = q\hbar N_2[\varphi_1(t;q), \varphi_2(t;q), \varphi_3(t;q)], \tag{17}$$

$$(1-q)\mathscr{L}[\varphi_3(t;q) - F_0(t)] = q\hbar N_3[\varphi_1(t;q), \varphi_2(t;q), \varphi_3(t;q)], \tag{18}$$

where $\mathscr{L}$ is the Laplace operator, subject to the initial conditions

$$\begin{aligned}
\varphi_1(0;q) &= T_0(0), \\
\varphi_2(0;q) &= I_0(0), \\
\varphi_3(0;q) &= F_0(0).
\end{aligned} \tag{19}$$

Clearly if $q = 0$ and $q = 1$ we obtain

$$\begin{aligned}
\varphi_1(t;0) &= T_0(t), \\
\varphi_1(t;1) &= T(t), \\
\varphi_2(t;0) &= I_0(t), \\
\varphi_2(t;1) &= I(t), \\
\varphi_3(t;0) &= F_0(t), \\
\varphi_3(t;1) &= F(t),
\end{aligned} \tag{20}$$

when q varies from zero to unity, the solution of the model (4)–(6) will vary from the initial guesses $T_0(t)$, $I_0(t)$, and

$F_0(t)$ to the exact solution $T(t)$, $I(t)$, and $F(t)$ of the model (4)–(6). Expanding $\varphi_i(t;q)$, $i = 1,2,3$ by the Taylor series with respect to the embedding parameter q yields

$$\varphi_1(t;q) = T_0(t) + \sum_{m=1}^{\infty} T_m(t) q^m, \tag{21}$$

$$\varphi_2(t;q) = I_0(t) + \sum_{m=1}^{\infty} I_m(t) q^m, \tag{22}$$

$$\varphi_3(t;q) = F_0(t) + \sum_{m=1}^{\infty} F_m(t) q^m, \tag{23}$$

where

$$\begin{aligned} T_m(t) &= \frac{1}{m!} \frac{\partial^m \varphi_1(t;q)}{\partial q^m}\Big|_{q=0}, \\ I_m(t) &= \frac{1}{m!} \frac{\partial^m \varphi_2(t;q)}{\partial q^m}\Big|_{q=0}, \\ F_m(t) &= \frac{1}{m!} \frac{\partial^m \varphi_3(t;q)}{\partial q^m}\Big|_{q=0}. \end{aligned} \tag{24}$$

The convergence of equations (21)–(23) depends on the nonzero auxiliary parameters $\hbar$ [20]. Moreover, if the initial values guessed for $T_0(t)$, $I_0(t)$, and $F_0(t)$ and the auxiliary parameter $\hbar$ are appropriately selected, then at $q = 1$, series (21)–(23) converges

$$\varphi_1(t;1) = T_0(t) + \sum_{m=1}^{\infty} T_m(t) \text{ i.e } \quad T(t) = T_0(t) + \sum_{m=1}^{\infty} T_m(t), \tag{25}$$

$$\varphi_2(t;1) = I_0(t) + \sum_{m=1}^{\infty} I_m(t) \text{ i.e } \quad I(t) = I_0(t) + \sum_{m=1}^{\infty} I_m(t), \tag{26}$$

$$\varphi_3(t;1) = F_0(t) + \sum_{m=1}^{\infty} F_m(t) \text{ i.e } \quad F(t) = F_0(t) + \sum_{m=1}^{\infty} F_m(t), \tag{27}$$

which must be one of the solution of model (4)–(6), as proved by [20]. The equations governing the unknown functions can be deduced from the zeroth-deformation equations (16)–(18). Define the vectors

$$\begin{aligned} \vec{T}_m(t) &= \{T_0(t), T_1(t), \ldots, T_m(t)\}, \quad m = 1,2,\ldots,n, \\ \vec{I}_m(t) &= \{I_0(t), I_1(t), \ldots, I_m(t)\}, \quad m = 1,2,\ldots,n, \\ \vec{F}_m(t) &= \{F_0(t), F_1(t), \ldots, F_m(t)\}, \quad m = 1,2,\ldots,n. \end{aligned} \tag{28}$$

Differentiating the zeroth-deformation equations (16)–(18) m-times with respect to the embedding parameter q, then setting $q = 0$, and finally dividing them by $m!$, enables the mth-order deformation equations to be obtained:

$$\mathcal{L}\left[T_m(t) - \chi_m T_{m-1}(t)\right] = \hbar R_{m,T}\left(\vec{T}_{m-1}, \vec{I}_{m-1}, \vec{F}_{m-1}\right), \quad m = 1,2,\ldots,n, \tag{29}$$

$$\mathcal{L}\left[I_m(t) - \chi_m I_{m-1}(t)\right] = \hbar R_{m,I}\left(\vec{T}_{m-1}, \vec{I}_{m-1}, \vec{F}_{m-1}\right), \quad m = 1,2,\ldots,n, \tag{30}$$

$$\mathcal{L}\left[F_m(t) - \chi_m F_{m-1}(t)\right] = \hbar R_{m,F}\left(\vec{T}_{m-1}, \vec{I}_{m-1}, \vec{F}_{m-1}\right), \quad m = 1,2,\ldots,n, \tag{31}$$

with initial conditions

$$\begin{aligned} T_m(0) &= 0, \\ I_m(0) &= 0, \\ F_m(0) &= 0. \end{aligned} \tag{32}$$

It should be emphasized that the mth-order deformation equations (29)–(31) are linear; hence, they can be solved by Mathematica or MATLAB. For simplicity, we can specify the auxiliary functions to be equal to unity. Applying the inverse Laplace transform to equations (29)–(31), we obtain

$$\begin{aligned} T_m(t) &= \chi_m T_{m-1}(t) + \hbar\, \mathcal{L}^{-1}\left(R_{m,T}\left(\vec{T}_{m-1}, \vec{I}_{m-1}, \vec{F}_{m-1}\right)\right), \quad m = 1,2,\ldots,n, \\ I_m(t) &= \chi_m I_{m-1}(t) + \hbar\, \mathcal{L}^{-1}\left(R_{m,I}\left(\vec{T}_{m-1}, \vec{I}_{m-1}, \vec{F}_{m-1}\right)\right), \quad m = 1,2,\ldots,n, \\ F_m(t) &= \chi_m F_{m-1}(t) + \hbar\, \mathcal{L}^{-1}\left(R_{m,F}\left(\vec{T}_{m-1}, \vec{I}_{m-1}, \vec{F}_{m-1}\right)\right), \quad m = 1,2,\ldots,n, \end{aligned} \tag{33}$$

where

$$R_{m,T}(t) = \mathscr{L}[T_{m-1}(t)] - (1-\chi_m)\left(T_0 + \frac{s\alpha t^\alpha}{M(\alpha)\Gamma(\alpha+1)} + \frac{s(1-\alpha)}{M(\alpha)}\right) - \frac{s^\alpha(1-\alpha)+\alpha}{s^\alpha M(\alpha)}\mathscr{L}$$
$$\cdot\left\{(\mu_T - k)T_{m-1}(t) + \frac{k}{T_{\max}}\sum_{i=0}^{m-1} T_i(t)T_{m-1-i}(t), + \frac{k}{T_{\max}}\sum_{i=0}^{m-1} T_i(t)I_{m-1-i}(t) + k_1\sum_{i=0}^{m-1} T_i(t)F_{m-1-i}(t)\right\},$$
$$R_{m,I}(t) = \mathscr{L}[I_{m-1}(t)] - (1-\chi_m)I_0 - \frac{s^\beta(1-\beta)+\beta}{s^\beta M(\beta)}\mathscr{L}\left(k_1'\sum_{i=0}^{m-1} F_i(t)T_{m-1-i}(t) - \mu_I I_{m-1}(t)_i\right), \tag{34}$$
$$R_{m,F}(t) = \mathscr{L}[F_{m-1}(t)] - (1-\chi_m)F_0 - \frac{s^\gamma(1-\gamma)+\gamma}{s^\gamma M(\gamma)}\mathscr{L}\left\{k_1\sum_{i=0}^{m-1} F_i(t)T_{m-1-i}(t) + \mu_F F_{m-1}(t) - M\mu_b I_{m-1}(t)\right\},$$
$$\chi_m = \begin{cases} 0, & m \le 1, \\ 1, & m > 1. \end{cases}$$

Next, the solution of the mth-order deformation equations (29)–(31) is given as

$$T_m(t) = (\chi_m + \hbar)T_{m-1}(t) - \hbar(1-\chi_m)\left(T_0 + \frac{s\alpha t^\alpha}{M(\alpha)\Gamma(\alpha+1)} + \frac{s(1-\alpha)}{M(\alpha)}\right) - \hbar\mathscr{L}^{-1}\frac{s^\alpha(1-\alpha)+\alpha}{s^\alpha M(\alpha)}\mathscr{L}$$
$$\cdot\left\{\left[(\mu_T - k)T_{m-1}(t) + \frac{k}{T_{\max}}\sum_{i=0}^{m-1} T_i(t)T_{m-1-i}(t) + \frac{k}{T_{\max}}\sum_{i=0}^{m-1} T_i(t)I_{m-1-i}(t) + k_1\sum_{i=0}^{m-1} T_i(t)F_{m-1-i}(t)\right]\right\}, \tag{35}$$
$$I_m(t) = (\chi_m + \hbar)I_{m-1}(t) - \hbar(1-\chi_m)I_0 - \hbar\mathscr{L}^{-1}\left\{\frac{s^\beta(1-\beta)+\beta}{s^\beta M(\beta)}\mathscr{L}\left[k_1'\sum_{i=0}^{m-1} F_i(t)T_{m-1-i}(t) - \mu_I I_{m-1}(t)\right]\right\}, \tag{36}$$
$$F_m(t) = (\chi_m + \hbar)F_{m-1}(t) - \hbar(1-\chi_m)F_0 - \hbar\mathscr{L}^{-1}\left\{\frac{s^\gamma(1-\gamma)+\gamma}{s^\gamma M(\gamma)}\mathscr{L}\left[k_1\sum_{i=0}^{m-1} F_i(t)T_{m-1-i}(t) + \mu_F F_{m-1}(t) - M\mu_b I_{m-1}(t)\right]\right\}. \tag{37}$$

Taking initial conditions and equations (35)–(37), we obtain

$$\begin{cases} T_1 = -\dfrac{\hbar}{M(\alpha)}\left(p + (k-\mu_T)T_0 + kT_0\left(1 - \dfrac{T_0+I_0}{T_{\max}}\right) - k_1T_0F_0\right)\left(1 - \alpha + \dfrac{\alpha t^\alpha}{\Gamma(1+\alpha)}\right), \\ I_1 = -\dfrac{\hbar(k_1'T_0F_0 - \mu_I I_0)}{M(\beta)}\left(1 - \beta + \dfrac{\beta t^\beta}{\Gamma(1+\beta)}\right), \\ F_1 = -\dfrac{\hbar(M\mu_b I_0 - k_1T_0F_0 - \mu_F F_0)}{M(\gamma)}\left(1 - \gamma + \dfrac{\gamma t^\gamma}{\Gamma(1+\gamma)}\right), \end{cases}$$

$$
\begin{aligned}
T_2 &= (1+\hbar)T_1 \\
&\quad + \frac{\hbar^2 m_1}{M(\alpha))^2}\left(k-\mu_T-\frac{k}{T_{\max}}(2T_0+I_0)-k_1F_0\right)\left(p+(k-\mu_T)T_0+kT_0\left(1-\frac{T_0+I_0}{T_{\max}}\right)-k_1T_0F_0\right) \\
&\quad - \frac{\hbar^2 k T_0 m_2}{M(\alpha)M(\beta)}\frac{(k_1'T_0F_0-\mu_I I_0)}{T_{\max}} \\
&\quad - \frac{\hbar^2 k_1 T_0 m_3}{M(\alpha)M(\gamma)}(M\mu_b I_0-k_1T_0F_0-\mu_F F_0), \\
I_2 &= (1+\hbar)I_1 \\
&\quad - \frac{\hbar^2 \mu_I m_4}{(M(\beta))^2}(k_1'T_0F_0-\mu_I I_0) \\
&\quad + \frac{\hbar^2 k_1' F_0 m_2}{M(\alpha)M(\beta)}\left(p+(k-\mu_T)T_0+kT_0\left(1-\frac{T_0+I_0}{T_{\max}}\right)-k_1T_0F_0\right) \\
&\quad + \frac{\hbar^2 k_1' T_0 m_5}{M(\gamma)M(\beta)}(M\mu_b I_0-k_1T_0F_0-\mu_F F_0), \\
F_2 &= (1+\hbar)F_1 \\
&\quad - \frac{\hbar^2 (k_1T_0+\mu_F)m_6}{(M(\gamma))^2}(M\mu_b I_0-k_1T_0F_0-\mu_F F_0) \\
&\quad - \frac{\hbar^2 k_1 F_0 m_3}{M(\alpha)M(\gamma)}\left(p+(k-\mu_T)T_0+kT_0\left(1-\frac{T_0+I_0}{T_{\max}}\right)-k_1T_0F_0\right) \\
&\quad + \frac{\hbar^2 M\mu_b m_5}{M(\gamma)M(\beta)}(k_1'T_0F_0-\mu_I I_0),
\end{aligned}
\tag{38}
$$

where $m_i, i = 1, 2, \ldots, 6$, are given by

$$
\begin{cases}
m_1 = (1-\alpha)^2 + \dfrac{2(1-\alpha)\alpha t^\alpha}{\Gamma(1+\alpha)} + \dfrac{(\alpha t^\alpha)^2}{\Gamma(2\alpha+1)}, \\
m_4 = (1-\beta)^2 + \dfrac{2(1-\beta)\beta t^\beta}{\Gamma(1+\beta)} + \dfrac{(\beta t^\beta)^2}{\Gamma(2\beta+1)}, \\
m_6 = (1-\gamma)^2 + \dfrac{2(1-\gamma)\gamma t^\gamma}{\Gamma(1+\gamma)} + \dfrac{(\gamma t^\gamma)^2}{\Gamma(2\gamma+1)}, \\
m_2 = (1-\alpha)(1-\beta) + \dfrac{(1-\alpha)\beta t^\beta}{\Gamma(1+\beta)} + \dfrac{(1-\beta)\alpha t^\alpha}{\Gamma(1+\alpha)} + \dfrac{\alpha\beta t^{\alpha+\beta}}{\Gamma(\alpha+\beta+1)}, \\
m_3 = (1-\alpha)(1-\gamma) + \dfrac{(1-\alpha)\gamma t^\gamma}{\Gamma(1+\gamma)} + \dfrac{(1-\gamma)\alpha t^\alpha}{\Gamma(1+\alpha)} + \dfrac{\alpha\gamma t^{\alpha+\gamma}}{\Gamma(\alpha+\gamma+1)}, \\
m_5 = (1-\beta)(1-\gamma) + \dfrac{(1-\beta)\gamma t^\gamma}{\Gamma(1+\gamma)} + \dfrac{(1-\gamma)\beta t^\beta}{\Gamma(1+\beta)} + \dfrac{\beta\gamma t^{\alpha+\gamma}}{\Gamma(\beta+\gamma+1)}.
\end{cases}
\tag{39}
$$

In a similar way, T_m, I_m, and F_m, for $m \geq 3$ can be obtained. Finally, the solution of model (2) is given by

$$T(t) = \sum_{m=0}^{n-1} T_m(t), \tag{40}$$

$$I(t) = \sum_{m=0}^{n-1} I_m(t), \tag{41}$$

$$F(t) = \sum_{m=0}^{n-1} F_m(t), \tag{42}$$

and by choosing a suitable value for $\hbar$ for the convergence of the series according to [20]. The analysis of the convergence of the HATM can found in the literature [35].

4. Numerical Illustration

According to [36], it should be noted that the solution of the series contain the auxiliary parameter $\hbar$, which offers an easy way to control the convergence of the solution of the series. Because it is essential to assure that the series equations (25)–(27) is convergent, we plotted the $\hbar$ curve of 6 terms of the FHATM solution for the fractional-time ABC equations in Figures 1–3. Using these $\hbar$ curves, we note that the straight line that parallels the $\hbar$ axis provides the region of convergence. These valid regions are listed in Table 2.

Furthermore, if $\hbar$ is appropriately chosen, equations (25)–(27) may converge fast. To this end, we have to compute the optimal values of the convergence control parameters from the minimum of the averaged residual errors.

Niu and Chun [37] introduced several methods to obtain the optimal value of $\hbar$. The optimal value of the convergence control parameter is defined by using the concept of the square residual error. An error analysis is presented to determine the optimal values of $\hbar$. We substitute equations (47)–(49) into equations (4)–(6) and obtain the residual functions as follows:

$$\begin{aligned} E_{m,T}(t;\hbar_1) = {}& {}_a^{\mathrm{ABC}}D_t^{\alpha}\psi_T(t;\hbar_1) - p + \mu_T\psi_T(t;\hbar_1) - k\psi_T(t;\hbar_1) \\ & \cdot\left(1 - \frac{\psi_T(t;\hbar_1) + \psi_I(t;\hbar_1)}{T_{\max}}\right) \\ & + k_1\psi_F(t;\hbar_1)\psi_T(t;\hbar_1), \end{aligned} \tag{43}$$

$$\begin{aligned} E_{m,I}(t;\hbar_2) = {}& {}_a^{\mathrm{ABC}}D_t^{\beta}\psi_I(t;\hbar_2) - k_1'\psi_F(t;\hbar_2)\psi_T(t;\hbar_2) \\ & + \mu_I\psi_I(t;\hbar_2), \end{aligned} \tag{44}$$

$$\begin{aligned} E_{m,F}(t;\hbar_3) = {}& {}_a^{\mathrm{ABC}}D_t^{\gamma}\psi_F(t;\hbar_3) - M\mu_b\psi_I(t;\hbar_3) \\ & + k_1\psi_F(t;\hbar_3)\psi_T(t;\hbar_3) + \mu_F\psi_F(t;\hbar_3). \end{aligned} \tag{45}$$

Then, the square residual error for the sixth-order approximation is defined as

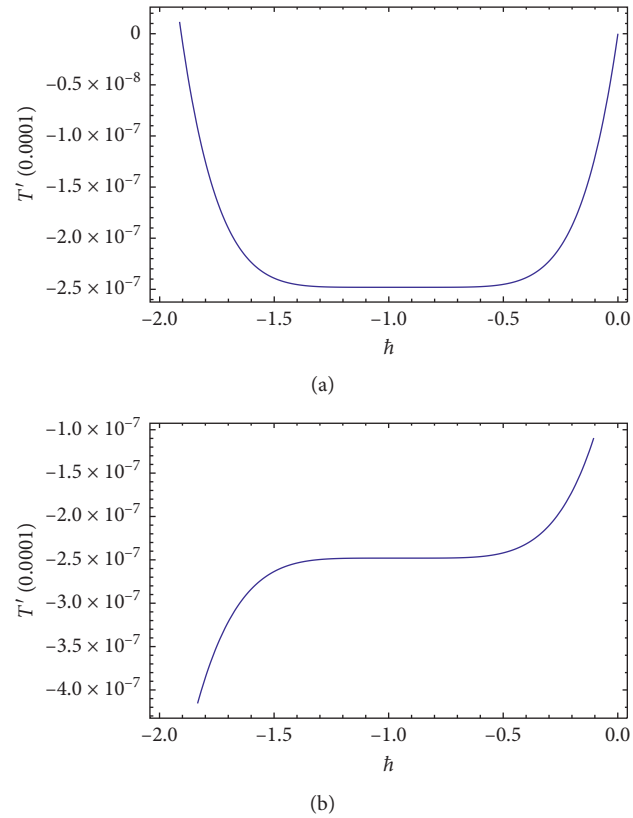

Figure 1: $\hbar$ curves obtained by the (a) 6th-order and (b) 5th-order approximation of the FHATM.

$$\begin{aligned} SE_{m,T}(\hbar_1) &= \frac{1}{(N+1)}\sum_{l=0}^{N}\left[E_{m,T}\left(\sum_{z=1}^{m} T(l\Delta t)\right)\right], \\ SE_{m,I}(\hbar_2) &= \frac{1}{(N+1)}\sum_{l=0}^{N}\left[E_{m,I}\left(\sum_{z=1}^{m} I(l\Delta t)\right)\right], \\ SE_{m,F}(\hbar_3) &= \frac{1}{(N+1)}\sum_{l=0}^{N}\left[E_{m,F}\left(\sum_{z=1}^{m} F(l\Delta t)\right)\right]. \end{aligned} \tag{46}$$

The use of the first derivative test enables us to determine the values of the auxiliary parameters $\hbar_1$, $\hbar_2$, and $\hbar_3$ for which $SE_{m,T}(\hbar_1)$, $SE_{m,I}(\hbar_2)$, and $SE_{m,F}(\hbar_3)$ are minimized. It should be emphasized that the approximation procedures that are used to select the optimal value of $\hbar$ in FHATM are similar to those of HAM [38].

In Table 3, the minimum values of the square residual error are given for the optimal values of $\hbar_1$, $\hbar_2$, and $\hbar_3$ when $\alpha = \beta = \gamma = 0.99$.

The absolute residual errors that were calculated for various $t \in (0, 1)$ are listed in Table 2. These results show that the FHATM obtains an accurate approximate solution for the fractional HIV model (4)–(6). The residual errors are plotted in Figure 4 for $t \in (0, 1)$ and various values of $\hbar$. The square residual errors are plotted in Figure 5, and Figure 6 shows the absolute residual

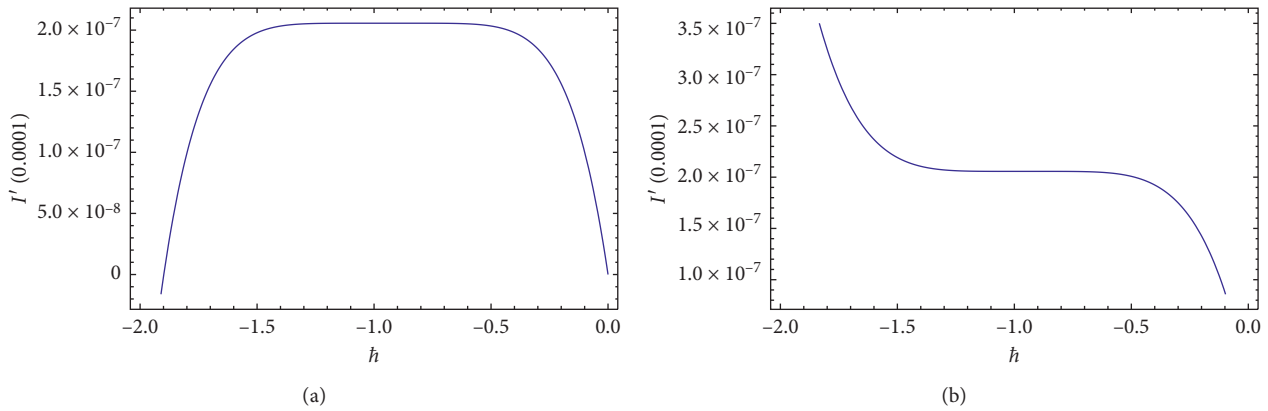

Figure 2: $\hbar$ curves obtained by the (a) 6th-order and (b) 5th-order approximation of the FHATM.

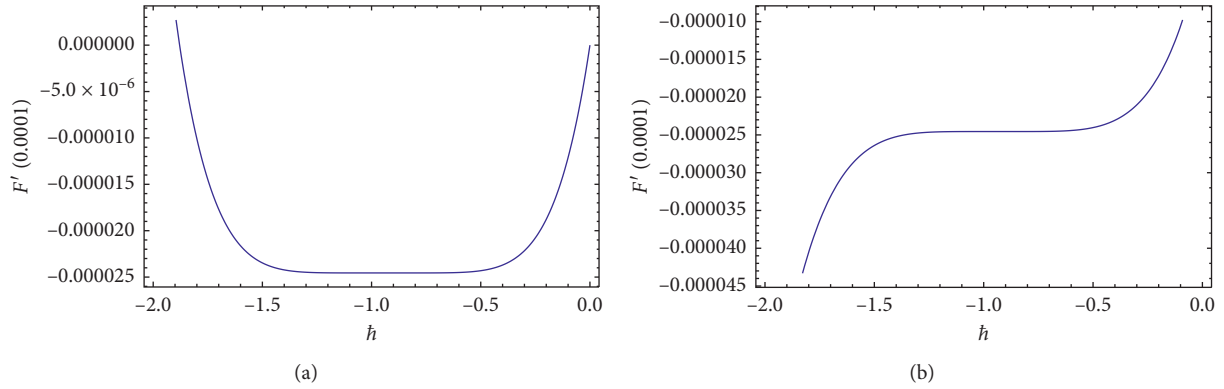

Figure 3: $\hbar$ curves obtained by the (a) 6th-order and (b) 5th-order approximation of the FHATM.

Table 2: Regions of convergence, optimal values of $\hbar$, and minimum values when $t = 0.0001$.

$\hbar$	$\hbar^*$	Minimum values
$-1.32 \le \hbar \le -0.62$	−0.804051	1.84022×10^{-11}
$-1.35 \le \hbar \le -0.65$	−0.805328	1.77401×10^{-11}
$-1.35 \le \hbar \le -0.65$	−0.808061	5.58464×10^{-7}

Table 3: Residual errors $E_{m,T}$, $E_{m,I}$, and $E_{m,F}$ for the optimal $\hbar$.

t	$E_{m,T}(t;\hbar_1^*)$	$E_{m,I}(t;\hbar_2^*)$	$E_{m,F}(t;\hbar_3^*)$
0	0.0000234312	0.0000194777	0.00234336
0.2	1.47222×10^{-8}	1.17419×10^{-8}	1.24526×10^{-6}
0.4	1.21518×10^{-8}	8.98671×10^{-9}	6.94956×10^{-7}
0.6	1.72222×10^{-8}	1.12419×10^{-8}	2.78878×10^{-7}
0.8	2.67042×10^{-8}	3.1236×10^{-8}	6.87927×10^{-6}
1	1.09289×10^{-8}	1.12475×10^{-8}	2.43936×10^{-6}

functions for the optimal $\hbar$. As these figures show, the solution obtained by using FHATM provides us with a sufficiently accurate analytical solution that only requires a few iterative steps. Mathematica software was used to calculate the six-term approximations for T, I, and F, respectively.

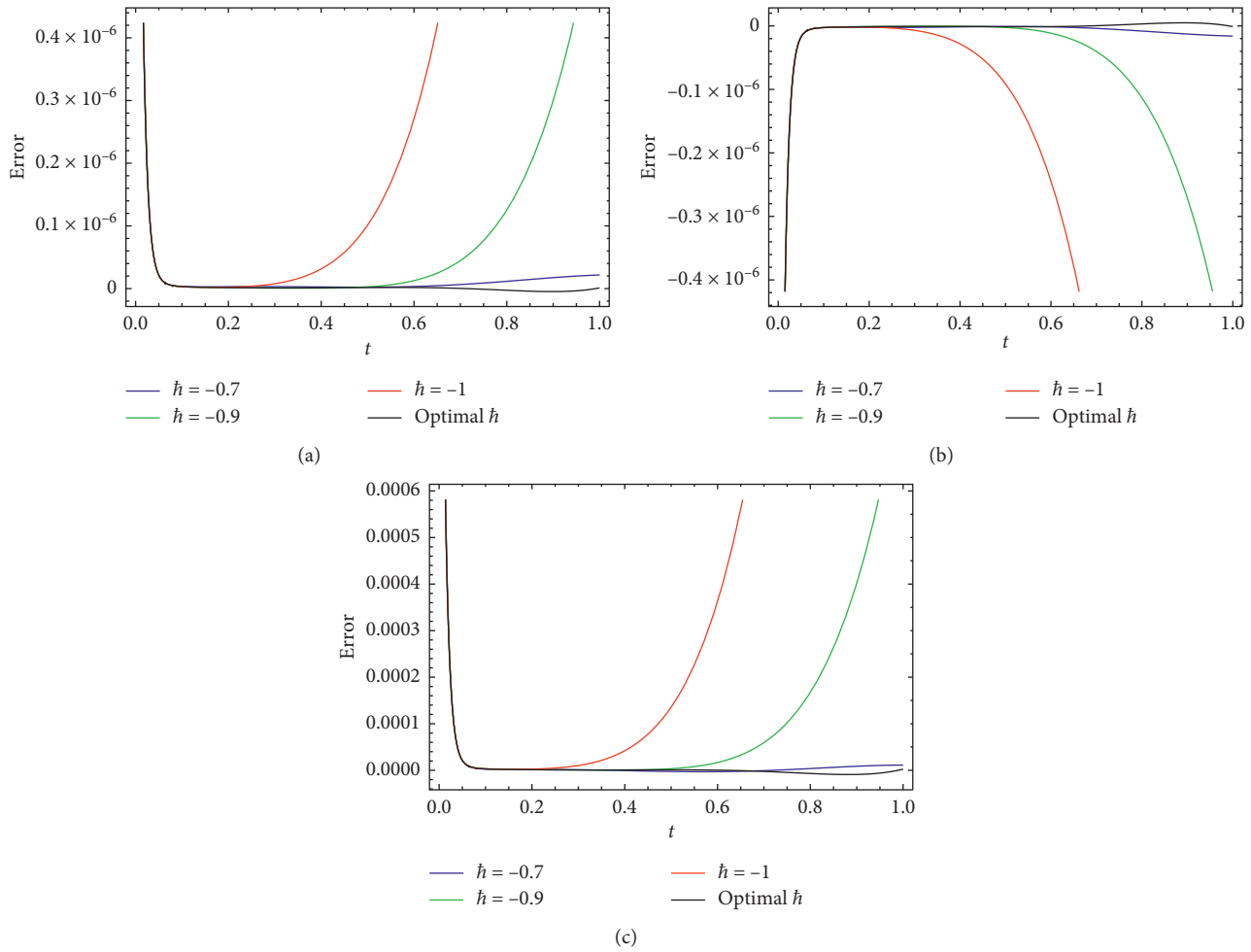

Figure 4: Errors of residual functions equations (39)–(41) using the sixth order of the approximation solution for various values of $\hbar$. (a) Comparison errors of residual function ET for various $\hbar$, (b) comparison errors of residual function EI for various $\hbar$, and (c) comparison errors of residual function EF for various $\hbar$.

$$\begin{aligned}\Upsilon_T(t;\hbar) = \sum_{m=0}^{6} T_m(t) &= 1000 + 1.44837\times10^{-6}\hbar + 3.70969\times10^{-6}\hbar^2 + 5.06867\times10^{-6}\hbar^3 \\ &+ 3.89645\times10^{-6}\hbar^4 + 1.59786\times10^{-6}\hbar^5 + 2.73079\times10^{-7}\hbar^6 + 0.000143992\hbar t^{0.99} \\ &+ 0.000377629\hbar^2 t^{0.99} + 0.000528248\hbar^3 t^{0.99} + 0.000415689\hbar^4 t^{0.99} + 0.000174472\hbar^5 t^{0.99} \\ &+ 0.0000305132\hbar^6 t^{0.99} + \cdots,\end{aligned} \tag{47}$$

$$\begin{aligned}\Upsilon_I(t;\hbar) = \sum_{m=0}^{6} I_m(t) &= -1.20698\times10^{-6}\hbar - 3.0988\times10^{-6}\hbar^2 - 4.24412\times10^{-6}\hbar^3 - 3.27012\times10^{-6}\hbar^4 \\ &- 1.34403\times10^{-6}\hbar^5 - 2.30202\times10^{-7}\hbar^6 - 0.000119993\hbar t^{0.99} - 0.000316179\hbar^2 t^{0.99} \\ &- 0.000444257\hbar^3 t^{0.99} - 0.000351059\hbar^4 t^{0.99} - 0.000147925\hbar^5 t^{0.99} - 0.0000259663\hbar^6 t^{0.99} - \cdots,\end{aligned} \tag{48}$$

$$\begin{aligned}\Upsilon_F(t;\hbar) = \sum_{m=0}^{6} F_m(t) &= 0.001 + 0.000146285\hbar + 0.000378272\hbar^2 + 0.000521647\hbar^3 + 0.000404615\hbar^4 \\ &+ 0.000167371\hbar^5 + 0.0000288456\hbar^6 + 0.0145431\hbar t^{0.99} + 0.0388549\hbar^2 t^{0.99}; \\ &+ 0.0552967\hbar^3 t^{0.99} + 0.0442161\hbar^4 t^{0.99} + 0.0188364\hbar^5 t^{0.99} + 0.00334019\hbar^6 t^{0.99} + \cdots.\end{aligned} \tag{49}$$

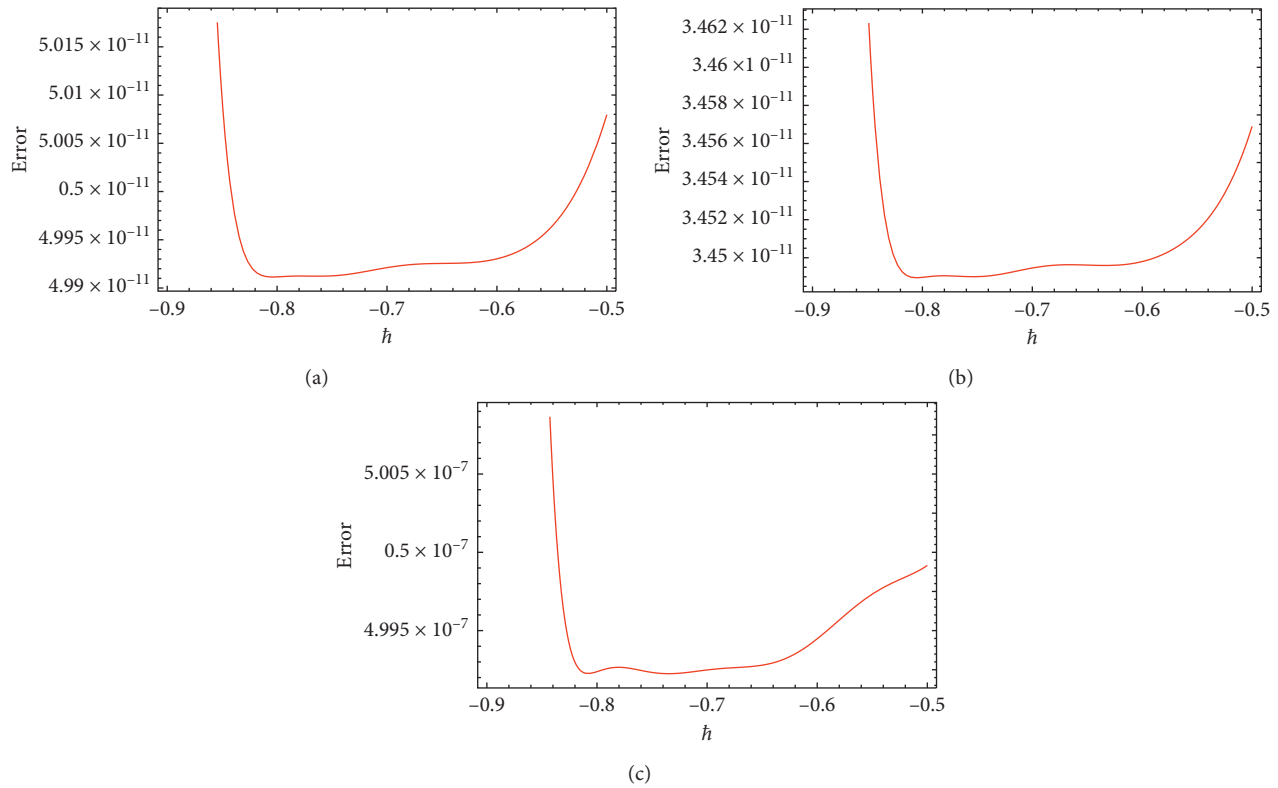

FIGURE 5: Square residual function equations (42)–(44) using the sixth order of the approximation solution for $\hbar \in (-0.9, -0.5)$. (a) Square residual errors of T versus $\hbar$, (b) square residual errors of I versus $\hbar$, and (c) square residual errors of F versus $\hbar$.

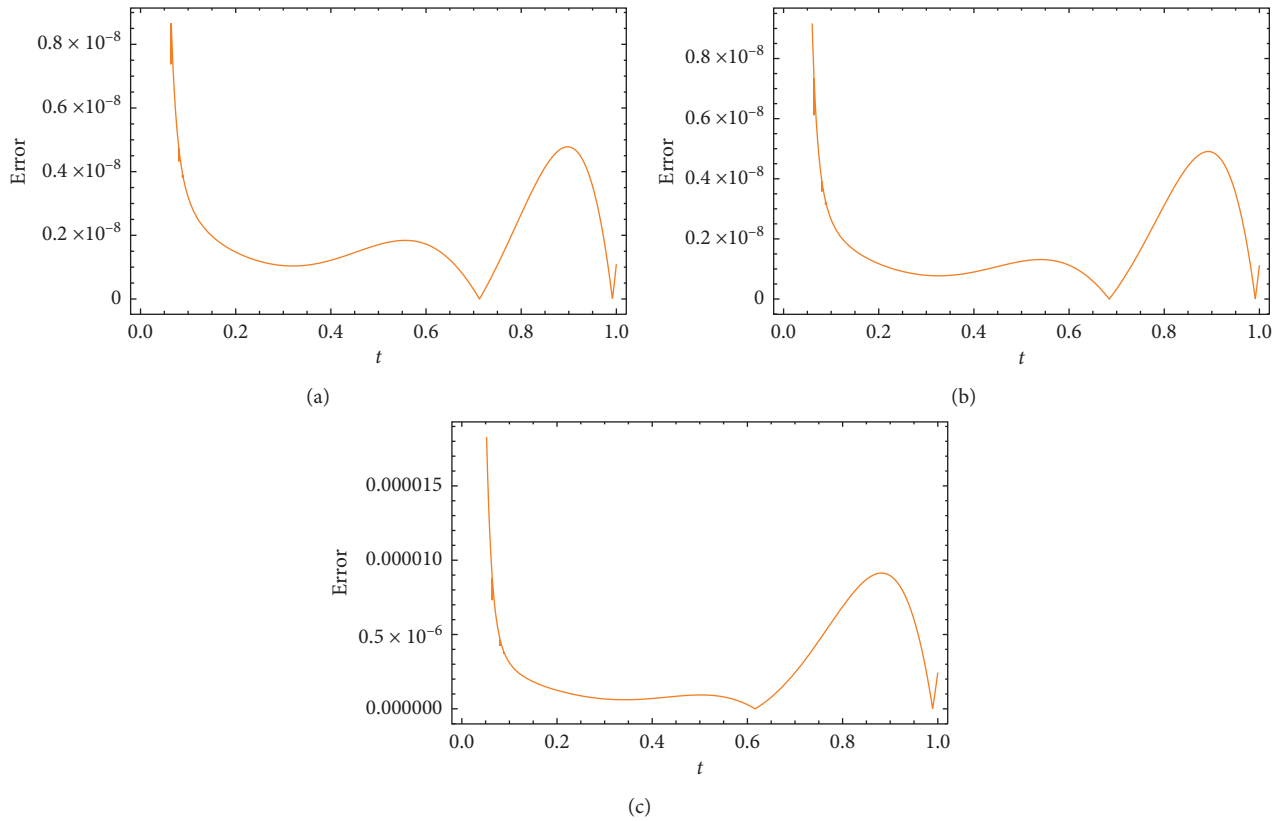

FIGURE 6: Absolute residual function equations (39)–(41) using the sixth order of the approximation solution for $\hbar^*$. (a) Absolute residual error functions for T and the optimal $\hbar$, (b) absolute residual error functions for I and the optimal $\hbar$, and (c) absolute residual error functions for F and the optimal $\hbar$.

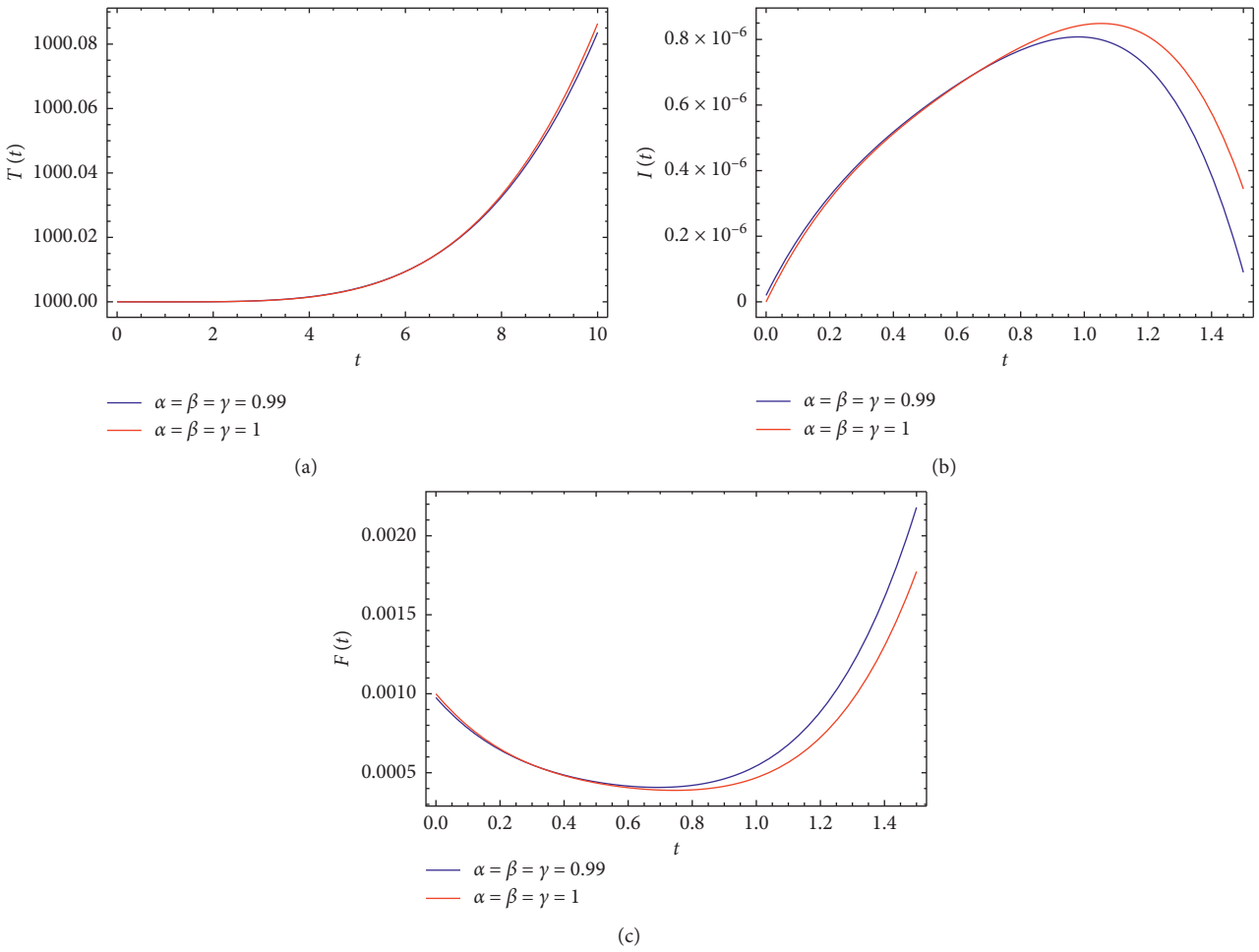

FIGURE 7: Numerical simulation of the concentrations of uninfected CD4$^+$ T cells $T(t)$, infected CD4$^+$ T cells $I(t)$, and HIV RNA $F(t)$ for different values of α, β, and γ and the optimal values of $\hbar^*$. (a) Approximate solut[[parms resize(1),pos(50,50),size(200,200),bgcol(156)]], and (c) approximate solutions of $F(t)$.

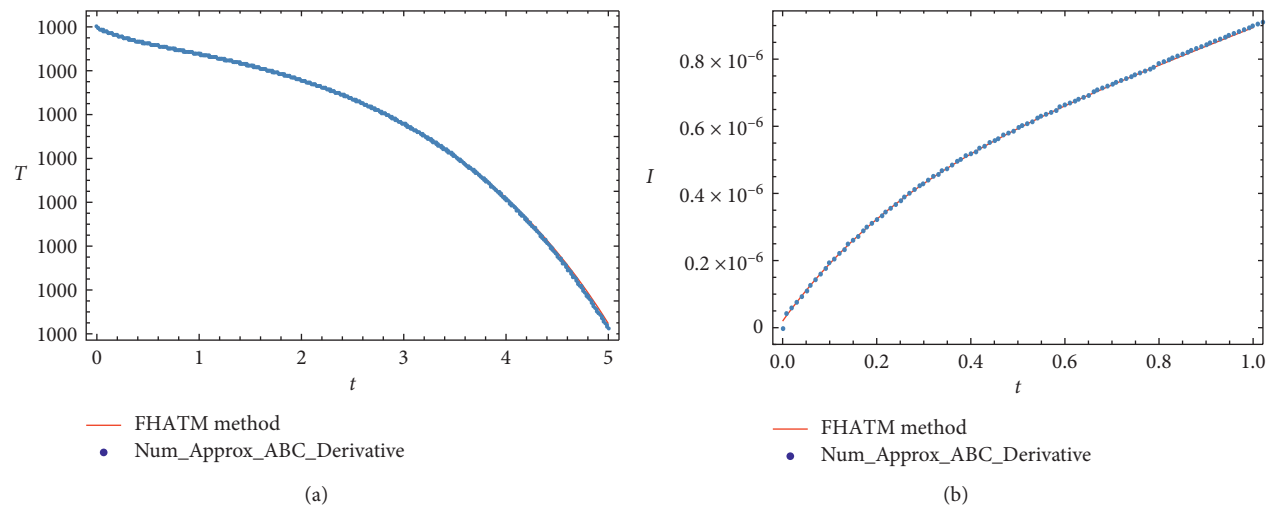

FIGURE 8: Continued.

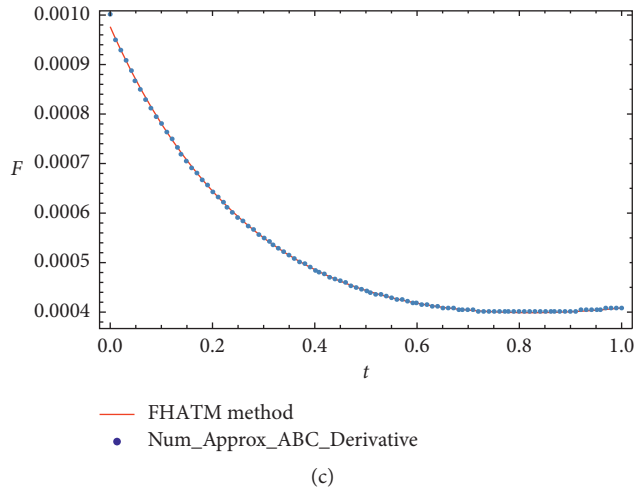

Figure 8: Comparison of the numerical solution with that obtained by FHATM for $\hbar = 0.01$. (a) Comparison of the numerical solution and FHATM solution for $\alpha = 0.99$, (b) comparison of the numerical solution and FHATM solution for $\beta = 0.99$, and (c) comparison of the numerical solution and FHATM solution for $\gamma = 0.99$.

Note that, if we set $\alpha = \beta = \gamma = 1$, then the FHATM solution is the same as that obtained with the HAM in [13]. The numerical results are plotted in Figure 7.

5. Numerical Scheme

In this section, we solve fractional a HIV model numerically using the numerical scheme introduced by Toufik and Atangana [27]. The numerical solution and FHATM solution are compared in Figure 8.

6. Conclusion and Further Work

In this study, we successfully solved the fractional HIV infection by using the $CD4^+$ T cells model numerically and analytically, which includes an operator of the type of the Atangana–Baleanu fractional derivative in the Caputo sense (ABC). Analytically approximate solution was obtained for this derivative by incorporating the FHATM in the model of the fractional HIV infection of $CD4^+$ T cells. The solution includes the auxiliary parameter $\hbar$, which provides an easy way to control the convergence region of the resulting infinite series. The results we obtained show that the FHATM is a successful technique for obtaining an approximate solution of the fractional HIV infection of $CD4^+$ T cells. Moreover, our result agrees strongly with the computation of Toufik and Atangana [27]. Studying the dynamics and stability of the system based on the ABC fractional definition and the FHATM algorithm is an interesting idea for the researchers.

Data Availability

No data were used.

Conflicts of Interest

The authors declare that they have no conflicts of interest.

References

[1] T. Abdeljawad, M. A. Hajji, Q. Al-Mdallal, and F. Jarad, "Analysis of some generalized abc-fractional logistic models," 2019, http://arxiv.org/abs/1912.08599.

[2] K. Ali Abro, "A fractional nd analytic investigation of thermo-diffusion process on free convection flow: an application to surface modification technology," *The European Physical Journal Plus*, vol. 135, no. 1, p. 31, 2020.

[3] K. A. Abro, I. A. Abro, and A. Yıldırım, "A comparative analysis of sulfate SO4−2 ion concentration via modern fractional derivatives: an industrial application to cooling system of power plant," *Physica A: Statistical Mechanics and its Applications*, vol. 541, Article ID 123306, 2020.

[4] K. Ali Abro and A. Atangana, "Role of non-integer and integer order differentiations on the relaxation phenomena of viscoelastic fluid," *Physica Scripta*, vol. 95, no. 3, Article ID 035228, 2020.

[5] K. Ali Abro, Ambreen Siyal, and A. Atangana, "Thermal stratification of rotational second-grade fluid through fractional differential operators," *Journal of Thermal Analysis and Calorimetry*, pp. 1–10, 2020.

[6] A. Atangana and B. Dumitru, "New fractional derivatives with nonlocal and non-singular kernel: theory and application to heat transfer model," 2016, http://arxiv.org/abs/1602.03408.

[7] R. L. Magin, *Fractional Calculus in Bioengineering*, Vol. 2, Begell House Redding, Redding, CA, USA, 2006.

[8] F. A. Rihan, Q. M. Al-Mdallal, H. J. AlSakaji, and A. Hashish, "A fractional-order epidemic model with time-delay and nonlinear incidence rate," *Chaos, Solitons & Fractals*, vol. 126, pp. 97–105, 2019.

[9] F. A. Rihan and G. Velmurugan, "Dynamics of fractional-order delay differential model for tumor-immune system," *Chaos, Solitons & Fractals*, vol. 132, Article ID 109592, 2020.

[10] M. M. Al-Sawalha, M. S. M. Noorani, and I. Hashim, "Numerical experiments on the hyperchaotic Chen system by the Adomian decomposition method," *International Journal of Computational Methods*, vol. 5, no. 3, pp. 403–412, 2008.

[11] I. Hashim, M. S. M. Noorani, R. Ahmad, S. A. Bakar, E. S. Ismail, and A. M. Zakaria, "Accuracy of the Adomian

decomposition method applied to the Lorenz system," *Chaos, Solitons & Fractals*, vol. 28, no. 5, pp. 1149–1158, 2006.

[12] A. K. Alomari, M. S. M. Noorani, and R. Nazar, "Solutions of heat-like and wave-like equations with variable coefficients by means of the homotopy analysis method," *Chinese Physics Letters*, vol. 25, no. 2, pp. 589–592, 2008.

[13] M. Ghoreishi, A. I. B. Md Ismail, and A. K. Alomari, "Application of the homotopy analysis method for solving a model for HIV infection of $CD4^+$ T-cells," *Mathematical and Computer Modelling*, vol. 54, no. 11-12, pp. 3007–3015, 2011.

[14] A. F. Jameel, N. R. Anakira, A. K. Alomari, M. A. Mahameed, and A. Saaban, "A new approximate solution of the fuzzy delay differential equations," *International Journal of Mathematical Modelling and Numerical Optimisation*, vol. 9, no. 3, pp. 221–240, 2019.

[15] D. Omari, A. K. Alomari, A. Mansour, A. Bawaneh, and A. Mansour, "Analytical solution of the non-linear michaelis–menten pharmacokinetics equation," *International Journal of Applied and Computational Mathematics*, vol. 6, no. 1, p. 10, 2020.

[16] N. R. Anakira, A. K. Alomari, A. F. Jameel, and I. Hashim, "Multistage optimal homotopy asymptotic method for solving boundary value problems with robin boundary conditions," *Far East Journal of Mathematical Sciences (FJMS)*, vol. 102, no. 8, pp. 1727–1744, 2017.

[17] M. S. H. Chowdhury, I. Hashim, and O. Abdulaziz, "Comparison of homotopy analysis method and homotopy-perturbation method for purely nonlinear fin-type problems," *Communications in Nonlinear Science and Numerical Simulation*, vol. 14, no. 2, pp. 371–378, 2009.

[18] B. Batiha, M. S. M. Noorani, and I. Hashim, "Application of variational iteration method to a general Riccati equation," *International Mathematical Forum*, vol. 2, no. 56, pp. 2759–2770, 2007.

[19] B. Batiha, M. S. Md Noorani, and I. Hashim, "Variational iteration method for solving multispecies Lotka–Volterra equations," *Computers & Mathematics with Applications*, vol. 54, no. 7-8, pp. 903–909, 2007.

[20] S. Liao, *Beyond Perturbation: Introduction to the Homotopy Analysis Method*, Chapman and Hall/CRC, Boca Raton, FL, USA, 2003.

[21] M. Khan and M. Hussain, "Application of Laplace decomposition method on semi-infinite domain," *Numerical Algorithms*, vol. 56, no. 2, pp. 211–218, 2011.

[22] S. Kumar, H. Kocak, and A. Yıldırım, "A fractional model of gas dynamics equations and its analytical approximate solution using Laplace transform," *Zeitschrift für Naturforschung A*, vol. 67, no. 6-7, pp. 389–396, 2012.

[23] M. Khan, M. A. Gondal, I. Hussain, and S. Karimi Vanani, "A new comparative study between homotopy analysis transform method and homotopy perturbation transform method on a semi infinite domain," *Mathematical and Computer Modelling*, vol. 55, no. 3-4, pp. 1143–1150, 2012.

[24] M. M. Khader, S. Kumar, and S. Abbasbandy, "New homotopy analysis transform method for solving the discontinued problems arising in nanotechnology," *Chinese Physics B*, vol. 22, no. 11, Article ID 110201, 2013.

[25] S. Kumar and M. M. Rashidi, "New analytical method for gas dynamics equation arising in shock fronts," *Computer Physics Communications*, vol. 185, no. 7, pp. 1947–1954, 2014.

[26] S. Kumar, J. Singh, D. Kumar, and S. Kapoor, "New homotopy analysis transform algorithm to solve Volterra integral equation," *Ain Shams Engineering Journal*, vol. 5, no. 1, pp. 243–246, 2014.

[27] M. Toufik and A. Atangana, "New numerical approximation of fractional derivative with non-local and non-singular kernel: application to chaotic models," *The European Physical Journal Plus*, vol. 132, no. 10, p. 444, 2017.

[28] I. Koca, "Modeling the heat flow equation with fractional-fractal differentiation," *Chaos, Solitons & Fractals*, vol. 128, pp. 83–91, 2019.

[29] S. A. A. Shah, M. A. Khan, M. Farooq, S. Ullah, and E. O. Alzahrani, "A fractional order model for Hepatitis B virus with treatment via Atangana-Baleanu derivative," *Physica A: Statistical Mechanics and its Applications*, vol. 538, p. 122636, 2020.

[30] P. Vázquez-Guerrero, J. F. Gómez-Aguilar, F. Santamaria, and R. F. Escobar-Jiménez, "Design of a high-gain observer for the synchronization of chimera states in neurons coupled with fractional dynamics," *Physica A: Statistical Mechanics and its Applications*, vol. 539, p. 122896, 2020.

[31] A. S. Perelson, "Modeling the interaction of the immune system with HIV," in *Mathematical and Statistical Approaches to AIDS Epidemiology*, pp. 350–370, Springer, Berlin, Germany, 1989.

[32] A. S. Perelson, D. E. Kirschner, and R. De Boer, "Dynamics of HIV infection of $CD4^+$ T cells," *Mathematical Biosciences*, vol. 114, no. 1, pp. 81–125, 1993.

[33] R. V. Culshaw and S. Ruan, "A delay-differential equation model of HIV infection of $CD4^+$ T-cells," *Mathematical Biosciences*, vol. 165, no. 1, pp. 27–39, 2000.

[34] T. Abdeljawad and Q. M. Al-Mdallal Al-Mdallal, "Discrete Mittag-Leffler kernel type fractional difference initial value problems and Gronwall's inequality," *Journal of Computational and Applied Mathematics*, vol. 339, pp. 218–230, 2018.

[35] S. Noeiaghdam and E. Khoshrouye Ghiasi, "Solving a nonlinear model of HIV infection for $CD4^+$ T cells by combining Laplace transformation and homotopy analysis method," 2018, http://arxiv.org/abs/1809.06232.

[36] M. M. Rashidi, S. A. Mohimanian pour, and S. Abbasbandy, "Analytic approximate solutions for heat transfer of a micropolar fluid through a porous medium with radiation," *Communications in Nonlinear Science and Numerical Simulation*, vol. 16, no. 4, pp. 1874–1889, 2011.

[37] Z. Niu and C. Wang, "A one-step optimal homotopy analysis method for nonlinear differential equations," *Communications in Nonlinear Science and Numerical Simulation*, vol. 15, no. 8, pp. 2026–2036, 2010.

[38] S. Liao, "An optimal homotopy-analysis approach for strongly nonlinear differential equations," *Communications in Nonlinear Science and Numerical Simulation*, vol. 15, no. 8, pp. 2003–2016, 2010.